A Novel Power Electronics-Based Fuel Cell Emulator

Siriroj Sirisukprasert[1] and **Trin Saengsuwan**[2], Non-members

ABSTRACT

This paper proposes a prototype of a new power electronics-based fuel cell emulator. It can effectively replace a real electrochemical fuel cell stack during the development stage of a fuel-cell based power generation. The power stage of this new fuel cell emulator consists of a current source converter (buck rectifier) and a dc-to-dc buck converter. The research mainly focuses on emulating the electrical behavior of two well-known fuel cell systems: Proton Exchange Membrane (PEM) and Solid Oxide fuel cells. A 1.5kW PEM fuel cell case is presented in this paper. Analysis, modeling and control strategy are presented. A hybrid control technique and a new voltage-current curve tracking technique have been proposed. Both static and dynamic performances of the proposed fuel cell emulator are experimentally verified. The results show that the proposed system can effectively perform in all three operation regions, i.e. activation, ohmic and concentration. With the collaboration of the power electronics circuits and the DSP-based controller, the proposed fuel cell emulator provides both precisely emulated voltage-current characteristic and high-quality output voltage and current.

Keywords: Fuel Cell, Fuel Cell Emulator, Fuel Cell Inverter

1. INTRODUCTION

Presently, fuel cell is one of the most promising renewable and sustainable power sources because of its high power density and very low emission. Fuel cells can be utilized as a clean power source for various applications such as portable electronic appliances, transportation, and residential building. In addition, the standalone aspect of distributed resource technology makes fuel cells particularly useful in remote areas, where are not served by the national power grid or where the national grid is unreliable and backup power is mandatory.

Manuscript received on February 2, 2009 ; revised on April 17, 2009.

[1,2] The authors are with The Department of Electrical Engineering, Faculty of Engineering, Kasetsart University, Bangkok, 10900, Thailand, Tel: +66(2)-942-8555 ext.1541, E-mail: fengsir@ku.ac.th

This research is supported by The Thailand Research Fund and Commission on Higher Education under grant no. MRG48-Siriroj Sirisukprasert.

There are, nowadays, six commercially available types of fuel cells, i.e. alkaline, direct methanol, molten carbonate, phosphoric acid, proton exchange membrane (PEM) and solid oxide (SO). Depended on applications, each type of these fuel cells has its own advantages over the others. PEM fuel cell, for example, is the most popular to be used in automotive applications due to its low operation temperature and high energy efficiency. While, the SO fuel cell is suitable for stationary power source application because of its high operation temperature, which can be used as a combined heat and power generator.

The output voltage of fuel cells is DC and is a function of the amount of load current and the fuel flow rate. The fuel cell voltage is directly proportional to the supplied fuel flow rate and is indirectly proportional to the load current. Moreover, the dynamic of fuel cell is considered too slow for general electrical load requirements. To fully utilize the energy from the fuel cell, a power management is, therefore, necessary. In general, a complete fuel cell power supply system consists of a fuel cell stack, a fuel supply system, a power electronic-based inverter and a master controller. In highly dynamic load fluctuation, the performance of a fuel cell system mainly relies on the characteristics of the inverter and a great response of the master controller. Thus, a fine tune process for the designed system plays an essential role. This process can be costly if the real fuel cell stack is used. Typically, the major cost of the development period of a fuel cell system is the fuel cell stack itself, because the life time of its membrane is quite limited at the moment, which is last approximately 1000 hours. Therefore, the main objective of this research is to develop an electrical power source such that it can be properly and efficiently replaced a real electrochemical fuel cell stack during the development period.

Several attempts to emulate electrical characteristic of fuel cells have been previously made. However, there are some disadvantages. The voltage of the DC link of circuit in [1] is quite high relatively to the output voltage, which can be varied from 20 V to 50 V. This means that the duty cycle for the buck converter is in the range of 0.06 to 0.16. Practically, such low duty cycles lower the entire system efficiency. This introduces an electromagnetic interference problem and stress on the main switching devices. In contrast, [2] applied basic electronics components such as bipolar junction transistors, diode and other passive components. The advantage of this kind of circuit is its

simplicity. However, the drawback is that the system is inflexible. The circuit must be entirely redesigned when a different type of fuel cell or operating points are selected. In [3], the system provides very precise fuel cell character. It can be used for various kinds of fuel cell. Nevertheless, the system implementation is somewhat questionable. The authors, therefore, proposes a new fuel cell emulator that solves those previous problems [4]. The main advantages of the proposed system are its flexibility to provide a wide range of operating point, high efficiency and simplicity in both control stage and power stage. Additionally, It can be precisely emulated the electrical behaviour for all those today commercially available fuel cell stacks.

2. ELECTRICAL CHARACTERISTIC OF FUEL CELLS

To explain the basic characteristics of fuel cells, PEM fuel cell is used as an example. A PEM fuel cell basically combines oxygen and hydrogen over a platinum catalyst to produce electrochemical energy. Only by products of this process are heat and water, which make the fuel cell a clean electrical power source. A voltage and current (V-I) characteristic of a conventional PEM fuel cells is shown in Fig. 1. The dash line in Fig. 1 shows the actual voltage-current characteristic of a single cell operating at room temperature and normal air pressure [5]. The variation of voltage for an individual cell is derived from the maximum cell voltage (sometimes called electromotive forces) and the different voltage loss states. The internal losses basically affects the voltage drop in an actual fuel cell that causes the cell voltage to be less than the no load voltage (ideal potential). These losses, which are also known as polarization or irreversibility, originate primarily from the following three electrochemical processes: 1) activation polarization, 2) ohmic polarization, and 3) concentration (mass transport) polarization.

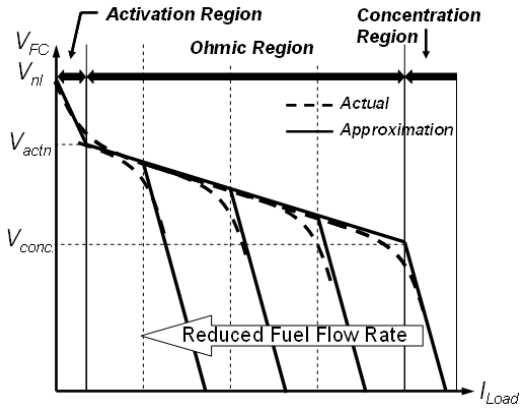

Fig.1: *Voltage-Current relationship of PEM fuel cell*

By using PEM fuel cell as an example, at a given temperature with partial pressure of the reactants and products known, the ideal voltage or no load potential is the maximum voltage that each cell in the stack can produce. Generally, the ideal terminal voltage of a PEM fuel cell can be calculated based on Gibbs free energy, and it is approximately 1.2 V at 25 C, where pure hydrogen and air are used.

The activation polarization occurs when the rate of the electrochemical reaction at an electrode surface is controlled by sluggish electrode kinetics. It is dominant at low current density. The higher load current, the higher activation loss. With the parasitic resistance of the polymer electrolyte membrane to the ions and the imperfect electrodes, the ohmic polarization loss is presented. In this region, the fuel cell terminal voltage linearly decreases with the increasing load. Concentration polarization (mass transportation) loss relates to the changes in the reactants concentration at the surface area of the electrodes as the fuel is being used. The concentration of the oxidant and the fuel is decreased at various points in the fuel-cell gas channels and is less than the concentration at the inlet value of the stack. This loss becomes significant at higher load currents when the fuel and the oxidant are used at higher rates, while the concentration in the gas channel is a minimum.

With acceptable accuracy, the V-I curve of a fuel cell can be approximated by three linear relationship corresponding to its irreversibility. The proposed fuel cell emulator thus approximates the actual behaviour of a fuel cell by the solid line shown in Fig. 1.

3. THE PROPOSED FUEL CELL EMULATOR

The proposed system consists of two main parts: power stage and control stage. Firstly, the detail of the power stage will be discussed. As shown in Fig. 2, the power stage is divided into two main parts: 1) a three-phase buck rectifier or a three-phase current source inverter (CSI) and 2) a buck converter or a step-down dc-to-dc converter. The input of the power stage is three-phase AC voltages, and its output is a DC voltage, which is able to follow the V-I characteristic of a selected fuel cells. Due to its higher power capability and its smaller DC voltage ripple compared to a single-phase supply. The three-phase CSI was selected as the front end of the proposed system. In comparison, a three-phase system can supply three times as much of maximum power and generates three times as high frequency voltage ripple as a single-phase does. Consequentially, a smaller DC link capacitor can be employed. Essentially, the buck rectifier converses a set of three-phase AC voltages to an adjustable DC voltage, which can be varied between 0 V and 0.866 V_p, where V_p is peak of the AC input line voltage. The very low duty cycle problem in [1] can be solved by using a stepped-down DC link in this stage. Basically, the DC link voltage of the

circuit is specifically set to fuel cell no-load voltage. This buck rectifier comprises 6 main switches (S_{BR1} to S_{BR6}) and 6 series diodes. Main function of the buck rectifier is to emulate the V-I characteristic of fuel cell when fuel (Hydrogen, for example) flow rate and pressure are adjusted as shown in Fig. 1. The concentration region is where the buck rectifier takes the action.

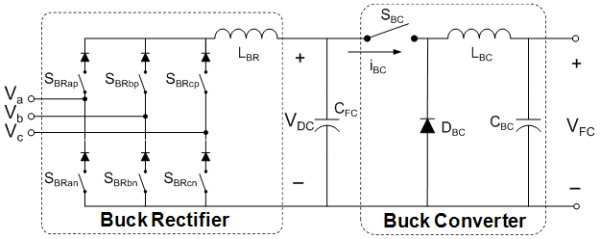

Fig.2: *Power stage of the proposed system*

To smooth the DC link voltage, an inductor, L_{BR}, and a capacitor, C_{FC}, are functioned as a low-pass filter. C_{FC} is additionally used as the intermediate energy storage. The dynamic characteristic of the output voltage and current can also be emulated by the buck rectifier.

The output end of the power stage for the proposed fuel cell emulator is a buck converter. The main function of the buck converter in this circuit is to generate the output DC voltage consistent with the V-I relationship in both activation and ohmic regions. The buck converter is composed of a main switch, S_{BC}, and free-wheeling diode, D_{BC}. The capacitor, C_{BC}, is used as a low-pass filter. The proposed V-I curve tracking technique will be used as a main algorithm to control the output of this buck converter.

4. POWER STAGE MODELING AND CONTROLLER DESIGN

A block diagram of the main controller of the proposed system is shown in Fig. 3. At the front end, two line-to-line input voltages are sensed for control synchronization. To control the output DC voltage, the output voltage, V_{FC}, and the output current, i_{Load}, are measured. A user command for this system is the flow rate of hydrogen, which is a main command of the buck rectifier. The outputs of the controller are switching signals for six switches of the buck rectifier and a switch for the buck converter.

4.1 Power Stage Modeling

Due to the large output voltage and output current variation, the feed-forward control technique is employed for the buck converter. However, to regulate V_{FC}, a closed-loop control on the buck rectifier is used to complete this task. To design the feedback control, the first step is to develop a small signal model for the buck rectifier. The following models are sequentially developed: a switching model, an average model in abc-coordinates, an average model in dq0-coordinates and a small-signal model in dq0-coordinates.

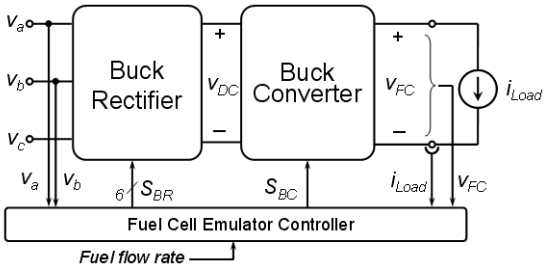

Fig.3: *Block diagram of the controller*

As shown in Fig. 3, the front end of the proposed system is a three-phase buck rectifier or known as a three-phase current source converter. Basically, the input of this buck rectifier are voltage controlled, while its output DC port is current controlled. The buck rectifier comprises six current-unidirectional, voltage-bidirectional switches, i.e. $S_{BRap}, S_{BRbp}, S_{BRcp}, S_{BRan}, S_{BRbn}$ and S_{BRcn}. Due to the current conduction constraint, the output current of buck rectifier must not be interrupted at any time. If a switching function "S" is defined as "1" and "0", when the corresponding main switch is turned "ON" and "OFF", respectively. For example, $S_{BRap} = 1$ if switch S_{BRap} is "ON", while $S_{BRap} = 0$, if switch S_{BRap} is "OFF". The following switching function can then be expressed:

$$S_{BRak} + S_{BRbk} + S_{BRck} = 1 \tag{1}$$

where, k is {p,n}.

From (1), the group of three top switches and the group of three bottom switches of the buck rectifier can then be modeled as two single-pole, triple-throw, current-unidirectional switches as shown in Fig. 4. As a result, the relationship of input and output of the buck rectifier can be obtained as follows:

$$v_{dc} = \vec{S}_{abc}^{T} \cdot \vec{v}_{abc} \tag{2}$$

$$\vec{i}_{abc} = \vec{S}_{abc} \cdot i_{dc} \tag{3}$$

Where,

$$\vec{i}_{abc} = \begin{bmatrix} i_a \\ i_b \\ i_c \end{bmatrix}, \vec{S}_{abc} = \begin{bmatrix} S_a \\ S_b \\ S_c \end{bmatrix} = \begin{bmatrix} S_{BRap} - S_{BRan} \\ S_{BRbp} - S_{BRbn} \\ S_{BRcp} - S_{BRcn} \end{bmatrix},$$

$$\text{and } \vec{v}_{abc} = \begin{bmatrix} v_a \\ v_b \\ v_c \end{bmatrix}$$

Applied (2) and (3) with the buck rectifier shown in Fig. 2, an average model in abc coordinate can be mathematically expressed as

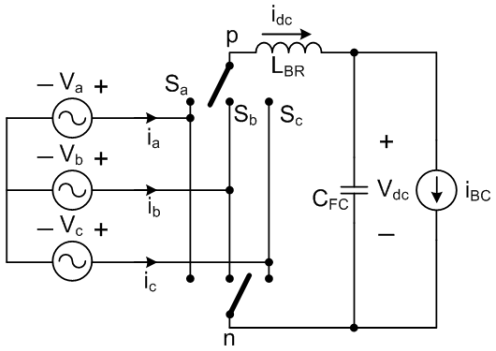

Fig.4: *A simplified switching model of the front-end buck rectifier*

$$\bar{\vec{i}}_{abc} = \vec{d}_{abc} \cdot \vec{i}_{dc} \tag{4}$$

$$(\vec{d}_{abc})^T \cdot \bar{\vec{v}}_{abc} = L_{BR}\frac{d\bar{i}_{dc}}{dt} + \bar{v}_{dc} \tag{5}$$

$$\bar{\vec{i}}_{abc} = C\frac{d\bar{v}_{dc}}{dt} + \bar{\vec{i}}_{BC} \tag{6}$$

where, the average value of the switching function is defined as a duty cycle, which can be expressed as follows:

$$\vec{d}_{abc} = \bar{\vec{S}}_{abc} = \frac{1}{T_S}\int_0^{T_s} \vec{S}_{abc}dt,$$

To achieve separated power control capability, the average model in abc coordinate is transformed to dq0 coordinate by employing well-known Park's transformation. Equations (4) thru (6) are then transformed into the following set of equations:

$$\bar{\vec{i}}_{dp0} = \vec{d}_{dp0} \cdot \bar{\vec{i}}_{dc} \tag{7}$$

$$(\vec{d}_{dp0})^T \cdot \bar{\vec{v}}_{dp0} = L_{BR}\frac{d\bar{i}_{dc}}{dt} + \bar{v}_{dc} \tag{8}$$

$$\bar{\vec{i}}_{abc} = C\frac{d\bar{v}_{dc}}{dt} + \frac{\bar{v}_{dc}}{R} \tag{9}$$

From (7) thru (9) and the well-known average model of buck converter, the average model of the proposed fuel cell emulator can be illustrated in Fig. 5. Since the balanced three-phase system is considered, the channel zero component can be omitted.

After applying the average operation followed by Park's transformation, a discrete time-varying power stage becomes a continuous time-invariant system in the dq0 space. This system can then be controlled by using the classical linear control theory. Based on a small-signal of the system, the control parameters can be derived. To further simplify the front end controller, the voltage vector in the abc space is arranged to inline with D axis as shown in Fig. 6. By doing

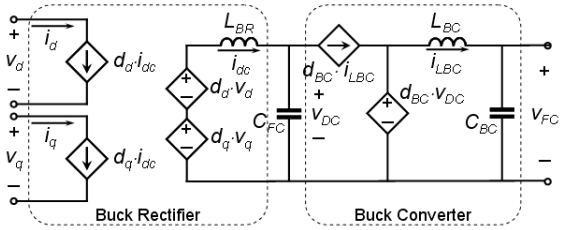

Fig.5: *An average model of the proposed power stage*

so, the quadrature components (Q channel) are eliminated. From the average model shown in Fig.5, the following relationship can be derived:

$$V_{DC} = d_d \cdot V_d \tag{10}$$

where, d_d is the direct-axis duty cycle of buck rectifier.

This means that the DC link can be adjusted by varying the direct-axis duty cycle, d_d. From Fig. 5 and (10), the steady-stage transfer function of the proposed power stage can simplified as follows:

$$V_{FC} = d_{BC} \cdot d_d \cdot V_d \tag{11}$$

where, d_{BC} is the duty cycle of buck converter.

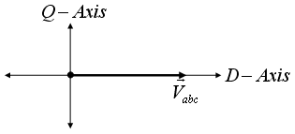

Fig.6: *Voltage vector in abc space inline with D axis*

4.2 Controller Design

As shown in Fig. 7, the proposed controller can be divided into 2 parts, i.e. buck converter controller and buck rectifier controller. The controller for buck rectifier is designed in such a way that its control response is much slower than the buck converter. The buck converter is working mostly in activation and ohmic regions, while the buck rectifier is working in the concentration region. In the activation and ohmic regions, the duty cycle d_d is kept constant. To avoid control interference between these two loops, the duty cycle d_{BC} maintains unchanged during the concentration region.

As mentioned previously, the buck converter is feed-forward controlled. The current, i_{Load}, V_d, d_d and the fuel flow rate command are fed into a look up table, LUT_{BC}. Without the DC link voltage sensor, the DC link can be approximated by multiplying Vd by d_d. The output of LUT_{BC} is the duty cycle for the buck converter is fed into the pulse width modulation (PWM) to generate the switching signal for the main switch, S_{BC}.

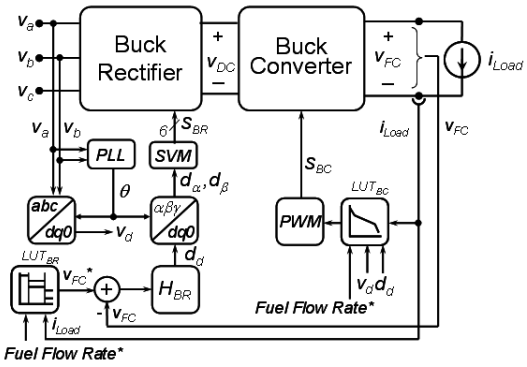

Fig.7: *Block diagram of the proposed controller*

The estimated technique used in the proposed system is shown by the solid line in Fig. 1. LUT_{BC} contains two linear relationships of fuel cell's output voltage and current, i.e., one for the activation region and the other one for the ohmic region. In most types of fuel cell stacks, the slope of the output voltage in the activation region is higher than that in the ohmic region. As shown in Fig.1, the slope for the activation region can be derived from V_{nl} and V_{actn}, while the slope for ohmic region can be derived from V_{actn} and V_{conc}. The different relationship of the voltage and the current in LUT_{BC} depends on the electrochemical characteristics of those fuel cells. Due to the feed-forward control, the voltage drop in the circuit is taken into account and is compensated in LUT_{BC}.

By utilizing dq0 control, two input phase voltages (V_a and V_b) are used as a three-phase synchronous signal. The phase lock loop (PLL) mathematically generates the angle of the input voltage vector, which is used in abc-to-dq0 transformation process. Another look up table applied in this control loop is LUT_{BR}. The fuel flow rate command and the load current are the inputs of this look up table. The output of LUT_{BR} is the voltage command, $V_{FC}{}^*$, which is compared with the feedback output voltage and the error is compensated by a PI controller (H_{BR}). Then, the command duty cycle, d_d, is derived. By using the inversed transformation matrix, d_d is converted to d_α and d_β. The 0-channel components are omitted based on the assumption of the balanced three-phase system. To generate switching signals for the buck rectifier, the space vector modulation (SVM) is employed.

5. THE PROPOSED V-I CURVE TRACKING TECHNIQUE

This section presents the proposed V-I curve tracking technique to be employed in the controller for the buck converter. The V-I characteristic of a 1.5kW PEM fuel cell stack from [3] is used as a reference. Fig. 8 depics the V-I curve of the PEM fuel cell with four different fuel flow rates, i.e. 100%, 75%, 50% and 25%. From Fig. 8, losses in a fuel cell known as polarization or irreversibility, originate primarily from three electrochemical processes: 1) activation polarization 2) ohmic polarization and 2) concentration (mass transport) polarization. The concept of the V-I curve tracking technique is to control the output power of the fuel emulator correspond to the output power of a real fuel cell at a particular fuel flow rate. From Fig. 8, the instantaneous output power of the referred PEM fuel cell is calculated and illustrated in Fig. 9. With a constant fuel flow rate, the output power of a fuel cell is approximately constant. The higher fuel flow rate, the higher maximum delivered output current.

A simple flowchart shown in Fig. 10 is the algorithm of V-I curve tracking method used in the proposed fuel cell emulator. The technique starts with reading output current (load current) and then calculate the output power. The calculated output power is then compared with its corresponding instantaneous output power as shown in Fig. 9. As a result, the duty cycle of the buck converter is decreased, if the generated output power of the fuel emulator is greater than rated instantaneous power. In contrast, if the output power is lower than the rated instantaneous power, the duty cycle will be increased.

In addition, as discussed previously, the fuel cells have a low dynamic range and slow transient response, which causes an unacceptable lag in responding to call for power by the controller [5]. This slow transient behavior is, therefore, taken into account in the proposed V-I curve tracking algorithm. This proposed fuel cell emulator can then be simulated the respond of output power interacted with additional battery or supercapacitors.

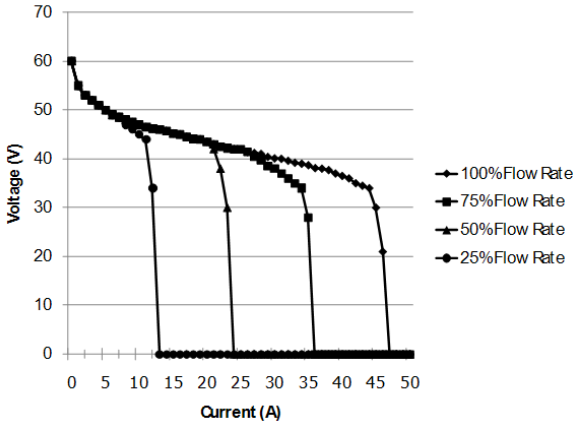

Fig.8: *Reference V-I characteristic of 1.5kW PEM fuel cell stack [3]*

6. SIMULATION RESULTS

To verify the static performance of the proposed system, the power stage and the controller (shown in

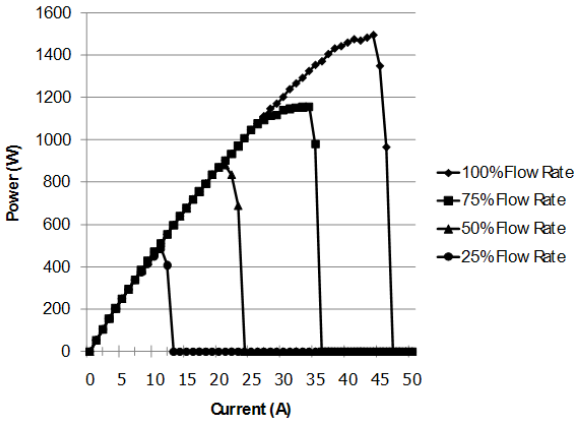

Fig.9: *The instantaneous power of the referred PEM fuel cell stack*

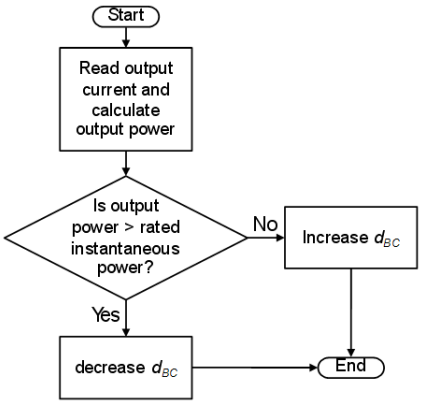

Fig.10: *Flowchart of proposed V-I curve tracking method*

Fig. 7) are simulated by MATLAB program. The main simulation parameters are shown in Table 1. A current source with 2A increment is used as the load. The load current is adjusted every 500 s. V-I characteristics from [3] is used as the reference. Typically, this kind of V-I curve can represent the output electrical characteristic for most types of today fuel cells. Four data sets used in the simulation are for the fuel flow rates of 25%, 50%, 75% and 100%. For 100% fuel flow rate, the fuel cell emulator terminal voltage at no load and full load is approximately 55 V and 22 V, respectively. The switching frequency of the buck converter is set to 30 kHz, which is about three times higher than that of the buck rectifier. To assure the performance of the controller, the bandwidth of control loop for the buck rectifier is about 1 kHz.

The simulation results for the fuel flow rates of 25%, 50%, 75% and 100% are shown in Fig.11 to Fig.14, respectively. Fig. 11 confirms that VFC is indirectly proportional to ILoad and effectively follows the referred V-I curve with 100% fuel flow rate. Figures 12 to 14 also show that the emulator can perform very well at other flow rates. However, overshoots of

Table 1: *Main parameters for the fuel cell emulator*

Parameters	Value
Power Stage	
- Buck rectifier switching frequency	10 kHz
- Buck converter switching frequency	30 kHz
- Input voltage	220 V - 3Φ
Fuel Cell Stack	
- Type of fuel cell stack	Proton Exchange Membrane Fuel Cell
- Maximum power	1.5 kW
- Terminal voltage range	22 V to 55 V
- V-I characteristic	Reference [3]

the emulator output voltage appears when its transfer from activation to ohmic, from ohmic to concentration and vice versa. This is because of the parasitic impedance in the circuit and the control bandwidth of the buck rectifier.

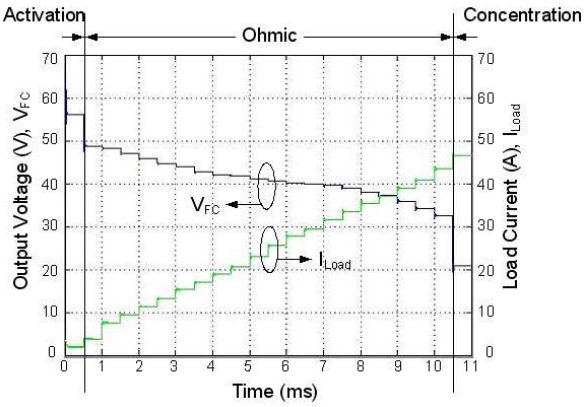

Fig.11: *V_{FC} as a function of load current at 100% fuel flow rate*

7. EXPERIMENTAL SETUP AND RESULTS

To further verify the performance of the proposed system, a hardware prototype of the fuel cell emulator has been implemented. The prototype consists of a power stage (Fig. 2) and a master controller. Each main switch (current-unidirectional, voltage-bidirectional switches) of the buck rectifier is implemented by an IGBT HGTG30N120CN in serried with a diode RHRG75120. A MOSFET STGP20NC60 and a diode RHRG75120 are used in the buck converter as a main switch and a free-wheeling diode, respectively. A 32-bit digital signal processor (DSP) TMS320F2812 is utilized as a main control unit of the master controller. To assure the performance of the controller, the bandwidth of control loop for the buck rectifier is about 1 kHz. A block diagram of the setup for the experiments is shown in Fig. 15. It

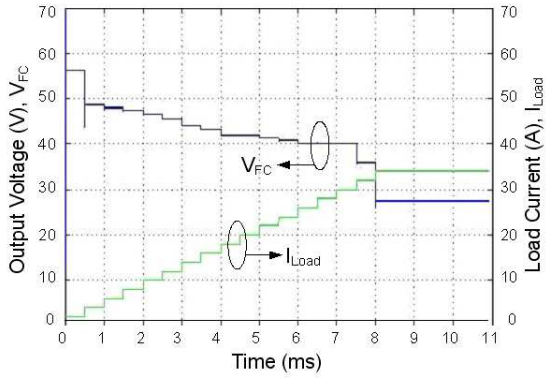

Fig.12: *V_{FC} as a function of load current at 75% fuel flow rate*

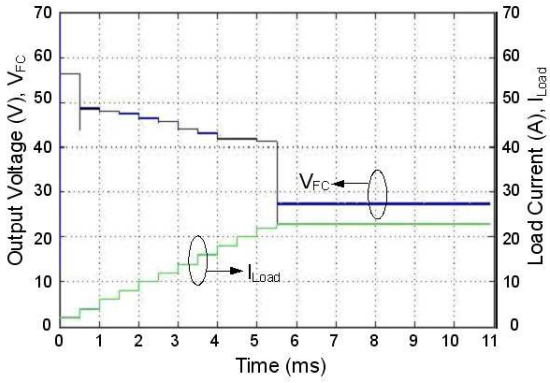

Fig.13: *V_{FC} as a function of load current at 50% fuel flow rate*

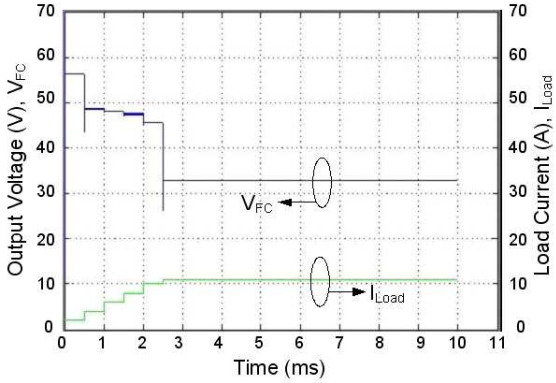

Fig.14: *V_{FC} as a function of load current at 25% fuel flow rate*

consists of the fuel cell emulator prototype, a 1.5kW laboratory-prototype inverter, a 3kW electronics load and a master controller. Fig. 16 illustrates a photograph of the hardware prototype of the fuel cell emulator and the inverter unit. The same setup parameters listed in Table 1 are used. As depicted in Fig. 8, the referred V-I characteristic is adapted from [3], which is experimentally collected from a 1.5kW PEM fuel cell unit. An input power of the system is 380V three-phase voltage source. The DC output voltage of the fuel cell emulator is fed to the inverter. The AC output of the inverter is then supplied to the electronic load. In the test setup, there are two input commands, which are the fuel flow rate and the load current for the electronic load.

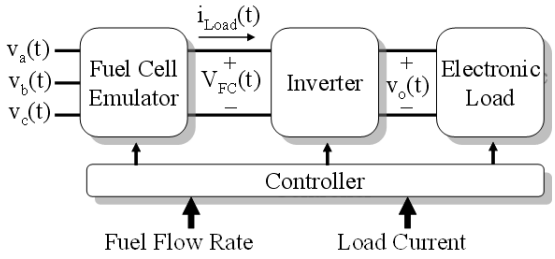

Fig.15: *Block diagram of the experimental setup*

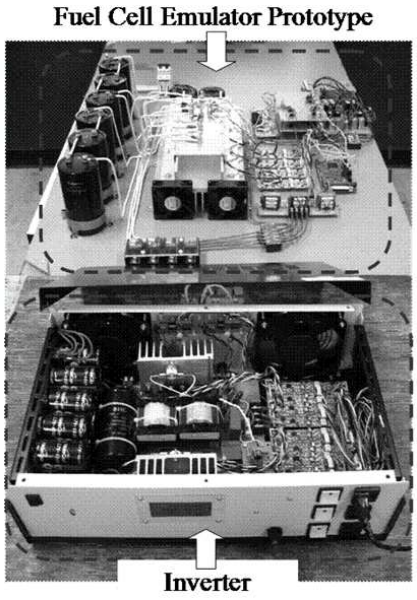

Fig.16: *Photograph of the hardware prototype*

The experiment is divided into two cases, i.e. 1) static test and 2) dynamic test. The objective of the static test is to verify that the fuel cell emulator can generate output voltage and supply load current according to the referred V-I curve at a constant fuel flow rate. For each fuel flow rate, the load current is varied by the electronic load. In this experiment, there are four levels of fuel flow rate, i.e. 100%, 75%, 50% and 25%.

The experimental results of the static test are shown in Figures 17 to 20. By using oscilloscope, the output voltage V_{FC}(t) of the fuel cell emulator is measured by channel 1, while the load current i_{Load}(t) is measured by channel 2. Employing X-Y plot function of the oscilloscope, i_{Load}(t) is set up as X-axis, and V_{FC}(t) is set up as Y-axis. In each fuel flow rate, a step-wise load current of the electronic load is varied with the period of 100 ms. The experimental V-I characteristic of the prototype by varying the load current with the fuel flow rate of 100%, 75%, 50% and 25% are shown in Fig. 17 thru 20, respectively.

The experimental results consistently agree with the reference V-I curves. However, in case of 100% fuel flow rate, V-I relationship is not linear due to the nonlinear behavior of the circuit and the bandwidth of the controller.

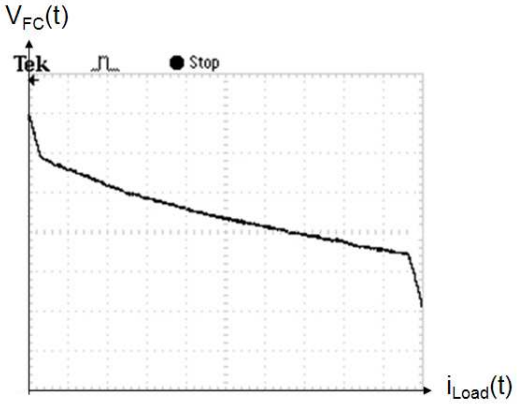

Fig.17: *V-I characteristics of the proposed fuel cell for fuel flow rate of 100% (XY-mode, V_{FC}(t): 10V/DIV, i_{Load}(t): 5A/DIV)*

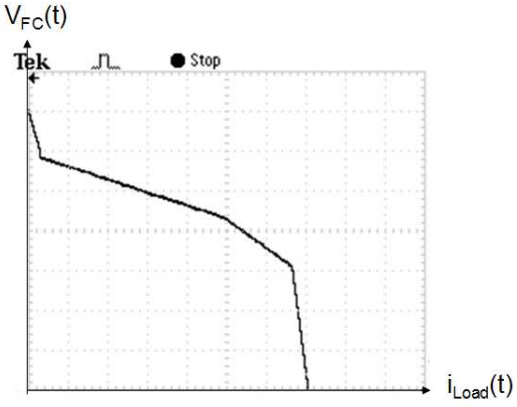

Fig.18: *V-I characteristics of the proposed fuel cell for fuel flow rate of 75% (XY-mode, V_{FC}(t): 10V/DIV, i_{Load}(t): 5A/DIV)*

The second test is to verify the dynamic respond and stability of the prototype. In this test, the fuel cell emulate is controlled to operate in two step loads,

Fig.19: *V-I characteristics of the proposed fuel cell for fuel flow rate of 50% (XY-mode, V_{FC}(t): 10V/DIV, i_{Load}(t): 5A/DIV)*

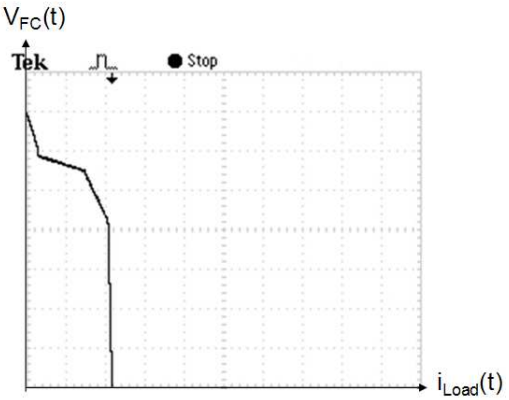

Fig.20: *V-I characteristics of the proposed fuel cell for fuel flow rate of 25% (XY-mode, V_{FC}(t): 10V/DIV, i_{Load}(t): 5A/DIV)*

i.e. no load and full load. These two step loads are switched back and forth every 20 ms (50 Hz). The experimental result is shown in Fig. 21. At no load, the emulator generates voltage of approximately 50 V with zero load current. At full load, the emulator supplies the load current of about 48 A with the output voltage of 26 V. The output power is approximate 1 kW. Note that it is not 1.5 kW, because the emulator operates in concentration region. The result also shows the slow respond of current and voltage of the emulator, which is embedded in the proposed V-I curve tracking algorithm. In conclusion, the experiment results indicate both precise static characteristic and stable dynamic responds.

8. CONCLUSIONS

This paper presented the detail of a new power electronics-based fuel cell emulator, which can be replaced a real fuel cell stack during the development stage of a fuel-cell inverter system. The main advantages of the proposed system are suitable to emu-

late behavior of various types of fuel cells, providing a clean output and simplicity in both control stage and power stage. The mathematical model of the power stage and the control strategy have been derived. The performance of the proposed circuit has been simulated and experimentally verified. With the collaboration of the DSP-based controller and the power electronics circuits, the proposed fuel cell emulator provides both precisely emulated voltage-current characteristic and high-quality output voltage and current. This verified that the proposed fuel cell emulator can effectively be a substitute of electrochemical fuel cell stack.

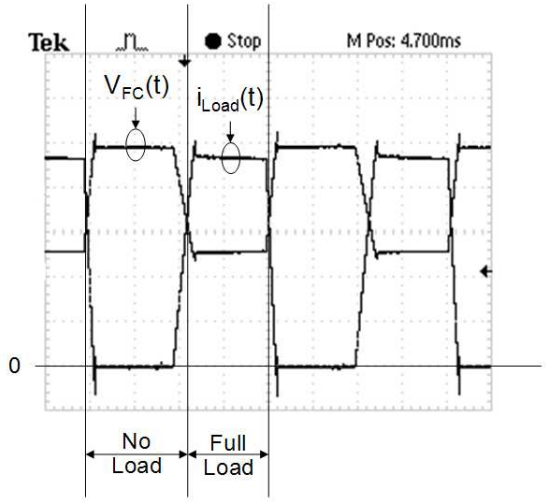

Fig.21: *Dynamic verification ($V_{FC}(t)$: 10V/DIV, $i_{Load}(t)$: 10A/DIV)*

9. ACKNOWLEDGEMENT

The authors would like to thank Professor Alex Q. Huang at North Carolina State University, USA, for the donated gate drivers and Professor Jason Lai at Virginia Tech, USA, for his useful comments. Sincerely thanks to Mr.Manoon Boonpramook and Mr.Wattana Samanjit, EE graduate students at Electrical Engineering Department, Kasetsart University, Thailand, for their contribution in this research.

This research is supported by The Thailand Research Fund and Commission on Higher Education under grant no. MRG48-Siriroj Sirisukprasert.

References

[1] T. W. Lee, S. H. Kim, Y. H. Yoon, S. J. Jang, C. Y. Won, "A 3 kW fuel cell generation system using the fuel cell simulator," *in Proc. IEEE International Symposium on Industrial Electronics*, vol. 2, pp. 833 - 837, 2004.

[2] S. Yuvarajan, Y. Dachuan, "Characteristics and modelling of PEM fuel cells," *in Proc. International Symposium on Circuits and Systems*, vol.5, pp. 880-883m, 2004..

[3] P. Famouri, R. S. Gemmen, "Electrochemical circuit model of a PEM fuel cell," *in Proc. IEEE Power Engineering Society General Meeting*, vol. 3, pp. 1436-1440, 2003.

[4] S. Sirisukprasert, T. Seangsuwan, "Power Electronics-based Fuel Cell Emulator," *in Proc. ECTI International Conference*, vol.1, pp. 281-284, 2007.

[5] National Energy Technology Laboratory, "Fuel Cell Hand Book (6th Edition)", Nov. 2002.

Siriroj Sirisukprasert received B.Eng. (Electrical Engineering) with 1st class honor from Kasetsart University, Bangkok, Thailand in 1996. He received his Master and Ph.D. degrees from Virginia Polytechnic Institute and State University (Virginia Tech), Blacksburg, Virginia, USA in 2000 and 2004, respectively. He is now an Assistant Professor at the Department of Electrical Engineering, Faculty of Engineering, Kasetsart University, Bangkok, Thailand. He is also the director of Kasetsart Applied Power Electronics Laboratory (KAPE LAB). His research interests include power electronics system, renewable energy management, power system quality and digital control design.

Trin Saengsuwan graduated in Electrical Engineering from Kasetsart University, Thailand, in 1984. He received the M.Sc. and Ph.D. degree from University of Manchester Institute of Science and Technology (UMIST), UK, in 1991 and 1995 respectively, UK. He is currently an Associate Professor at the Department of Electrical Engineering, Faculty of Engineering, Kasetsart University, Bangkok, Thailand. His main research areas of interests are transients simulations, power system protections, power quality and power system analysis.